Supplement of Nat. Hazards Earth Syst. Sci., 26, 3881–3900, 2026
https://doi.org/10.5194/nhess-26-3881-2026-supplement

Natural Hazards and Earth System Sciences
Open Access

Supplement of

Projecting changes in rainfall-induced landslide susceptibility across inhabited areas of China under climate change

Jinqi Wang et al.

Correspondence to: Kai Liu (liukai@bnu.edu.cn)

Supplementary Table

Supplementary Table S1: Comparison of simulated precipitation and observed precipitation (The root mean square error (RMSE) for different models)

ID	Model	RMSE	Mean RMSE (574.60)
1	IPSL-CM6A-LR	561.81	RMSE ≤ Mean RMSE
2	BCC-CSM2-MR	567.90	
3	MPI-ESM1-2-HR	568.80	
4	INM-CM5-0	568.86	
5	ACCESS-CM2	569.07	
6	NESM3	569.17	
7	CanESM5	569.96	
8	UKESM1-0-LL	570.11	
9	CNRM-ESM2-1	570.14	
10	KIOST-ESM	570.22	
11	EC-Earth3	570.34	
12	HadGEM3-GC31-LL	570.76	
13	EC-Earth3-Veg-LR	570.87	
14	CNRM-CM6-1	571.33	
15	MIROC-ES2L	571.73	
16	FGOALS-g3	571.80	
17	GISS-E2-1-G	572.02	
18	NorESM2-LM	572.61	
19	ACCESS-ESM1-5	573.04	
20	INM-CM4-8	573.18	
21	MRI-ESM2-0	575.14	RMSE ≥ Mean RMSE
22	IITM-ESM	576.75	
23	MPI-ESM1-2-LR	577.33	
24	GFDL-ESM4	577.53	
25	NorESM2-MM	577.96	
26	MIROC6	578.38	
27	CESM2	579.36	
28	CMCC-ESM2	580.93	
29	TaiESM1	581.35	
30	CMCC-CM2-SR5	596.12	
31	KACE-1-0-G	607.04	

Notes:

(1) RMSE is calculated using the formula provided above, which compares simulated and observed annual precipitation totals for each model.

(2) Mean RMSE is 574.60, representing the average RMSE across all models.

(3) Models with an RMSE ≤ mean RMSE are considered to have better simulated accuracy relative to the overall dataset.

Formula:

The RMSE is calculated as follows:

$$RMSE = \sqrt{\frac{1}{n}\sum_{i=1}^{n}(O_i - P_i)^2}$$

Where:

(1)n is the number of grid cells (pixels) in the raster,

(2)O_i is the observed precipitation at the $i - th$ grid cell,

(3)P_i is the predicted precipitation at the $i - th$ grid cell.

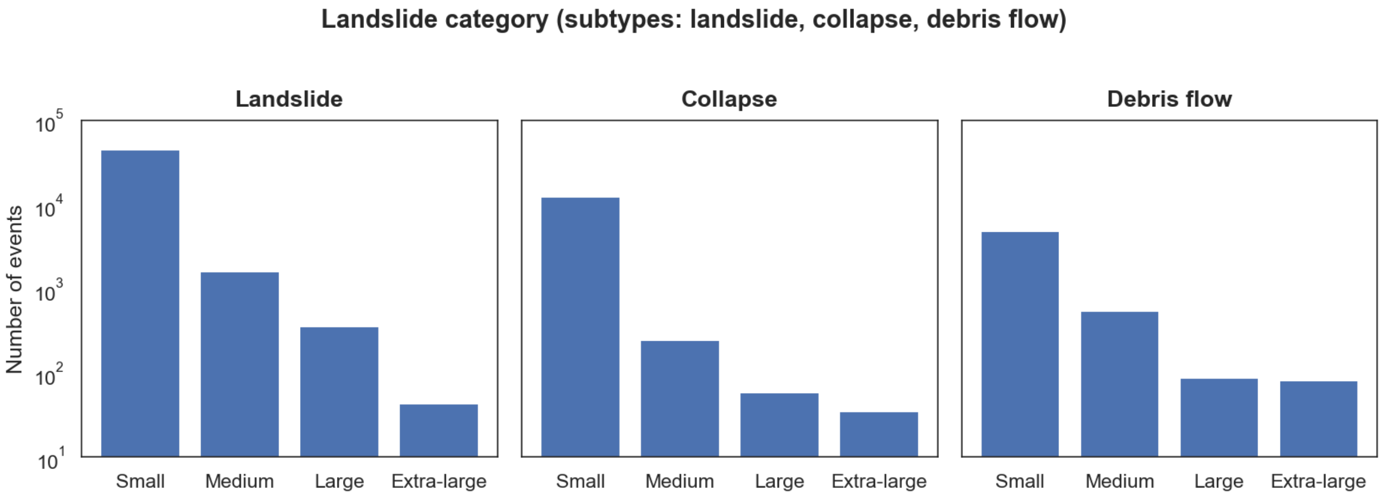

Supplementary Figure. S1: From 2008 to 2023 in China, rainfall-induced landslide-related hazards (here treated as a broad landslide category that includes landslides, collapses, and debris flows) show a clear small-to-medium dominance. Among the three subtypes, landslides are the most frequent, and are overwhelmingly concentrated in the small class. Collapses and debris flows occur less often overall, but they follow the same pattern, with most events falling into the small and medium classes. Event counts decline sharply with increasing scale across all subtypes, and large to extra-large events are comparatively rare. Overall, the 2008 – 2023 record indicates that China's rainfall-induced landslide-related hazards are characterized by high-frequency, smaller-scale events, with extreme large events occurring infrequently.

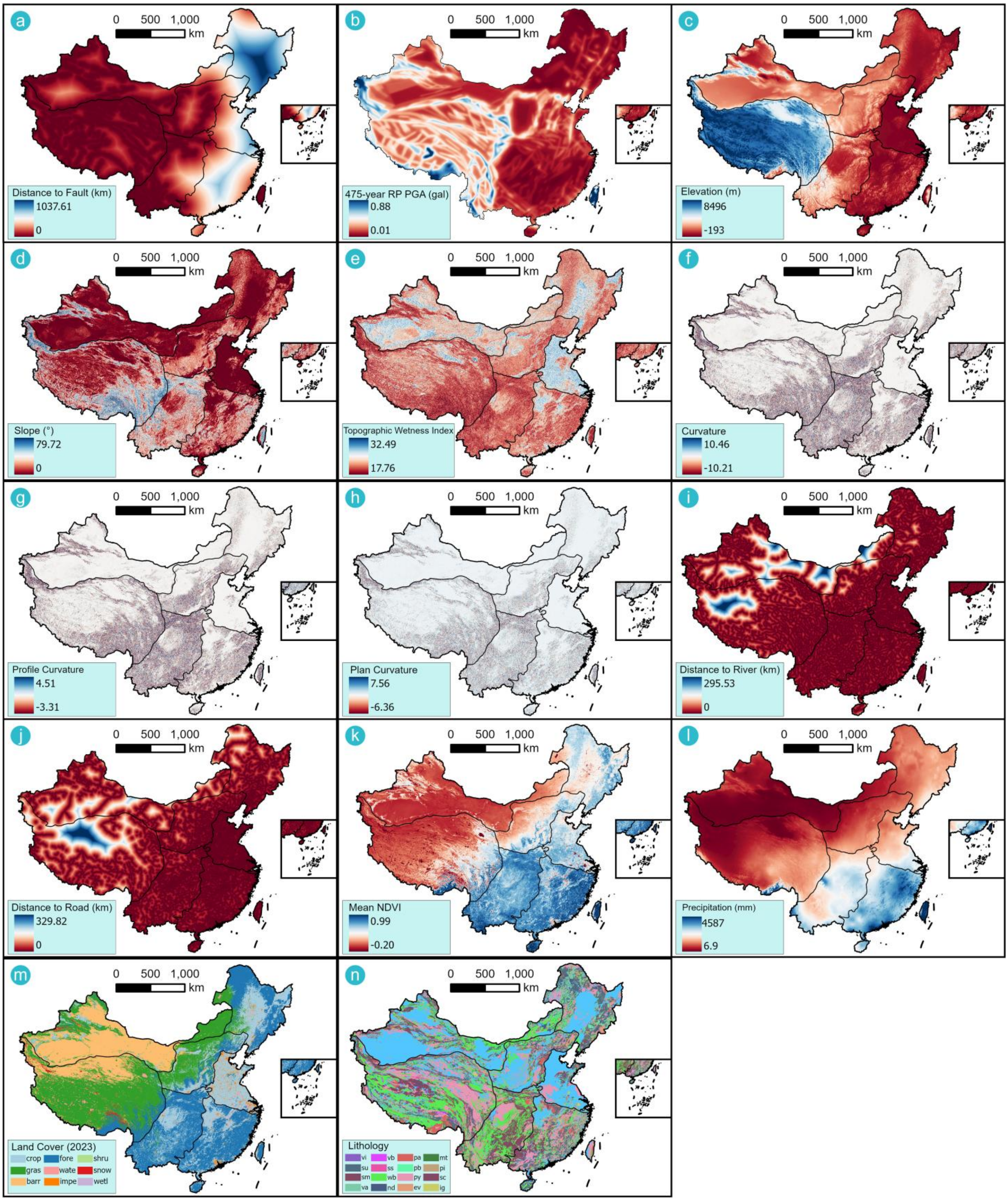

Supplementary Figure. S2: Landslide influencing factors utilised in this study. (a) Distance to fault, (b) PGA with a 475-year return period, (c) Elevation, (d) Slope, (e) Topographic Wetness Index (TWI), (f) Curvature, (g) Profile Curvature, (h) Plan Curvature, (i) Distance to River, (j) Distance to Road, (k) Mean NDVI: Monthly mean NDVI from 2008 to 2023, (l) Precipitation: Annual total precipitation, (m) Land cover. crop: Cropland, fore: Forest, shru: Shrub, gras: Grassland, wate: Water, snow: Snow/Ice, barr: Barren, impe: Impervious, wetl: Wetland. (n) Lithology. ev: evaporites, sc: carbonate sedimentary rocks, ig: ice and glaciers, sm: mixed sedimentary rocks, mt: metamorphics, ss:

siliciclastic sedimentary rocks, nd: no data, su: unconsolidated sediments, pa: acidic plutonic rocks, va: acidic volcanic rocks, pb: basic plutonic rocks, pi: intermediate plutonic rocks, vi: intermediate volcanic rocks, py: pyroclastics, wb: water bodies.

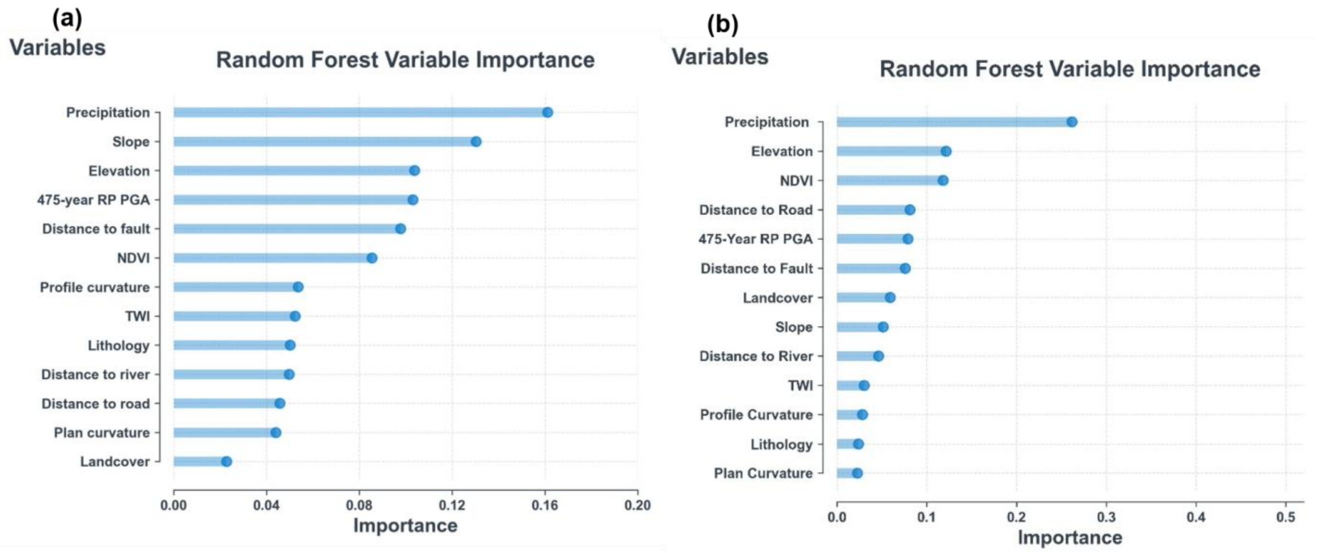

Supplementary Figure. S3: Relative importance of landslide conditioning factors as determined by the random forest (RF) model. (a) Feature importance derived using non-landslide samples generated in areas with human presence. (b) Feature importance derived using non-landslide samples randomly generated across the whole study area.

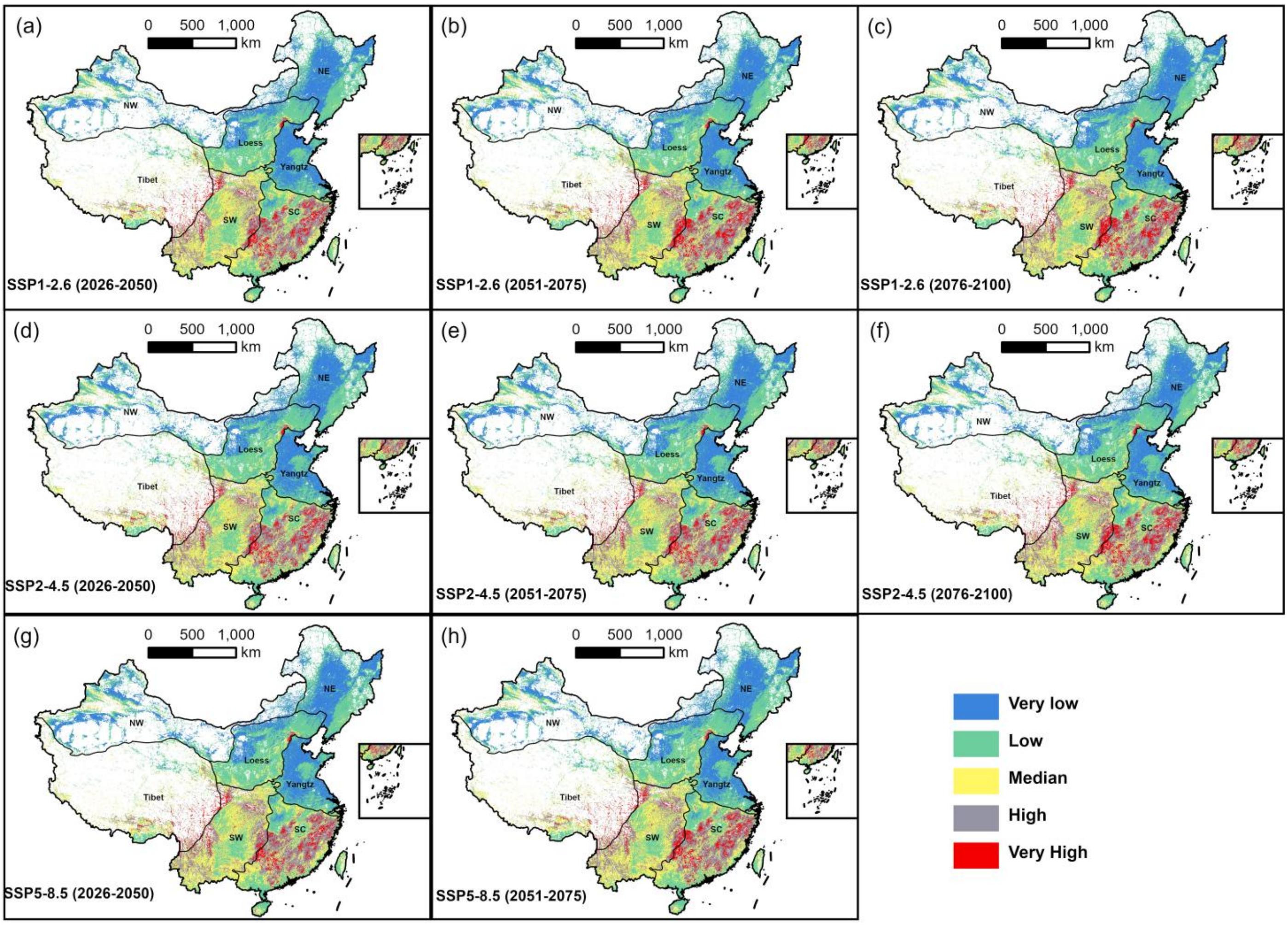

Supplementary Figure. S4: Spatial pattern of landslide susceptibility within inhabited areas of China during future periods: near-term future (2026–2050), mid-term future (2051–2075), and long-term future (2076–2100) under SSP1-2.6, SSP2-4.5, and SSP5-8.5.

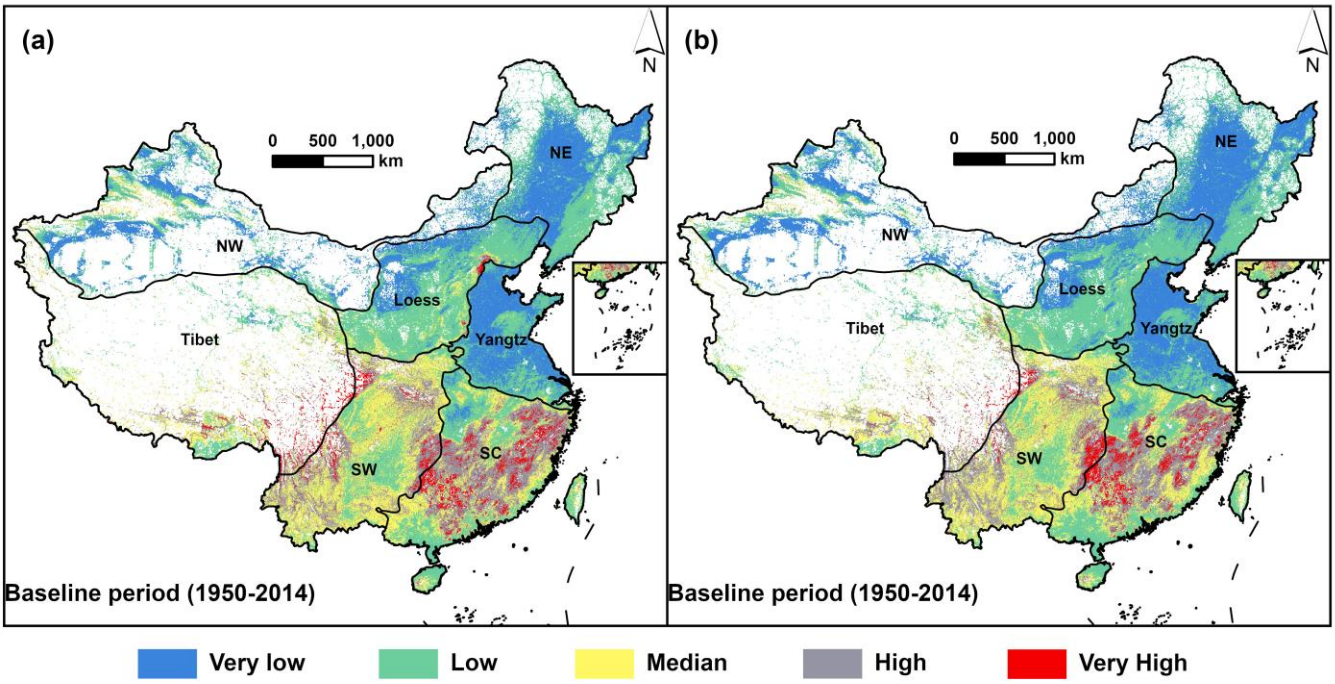

Supplementary Figure. S5: Landslide susceptibility mapping within inhabited areas of China for the baseline period (1950 - 2014). (a) Combined susceptibility map representing landslides, rockfalls, and debris flows as defined in this study (AUC = 0.96). (b) Susceptibility map for landslides only, excluding rockfalls and debris flows (AUC = 0.96). The Pearson correlation coefficient between the two models is 0.924, with a Mean Squared Error (MSE) of 0.187.

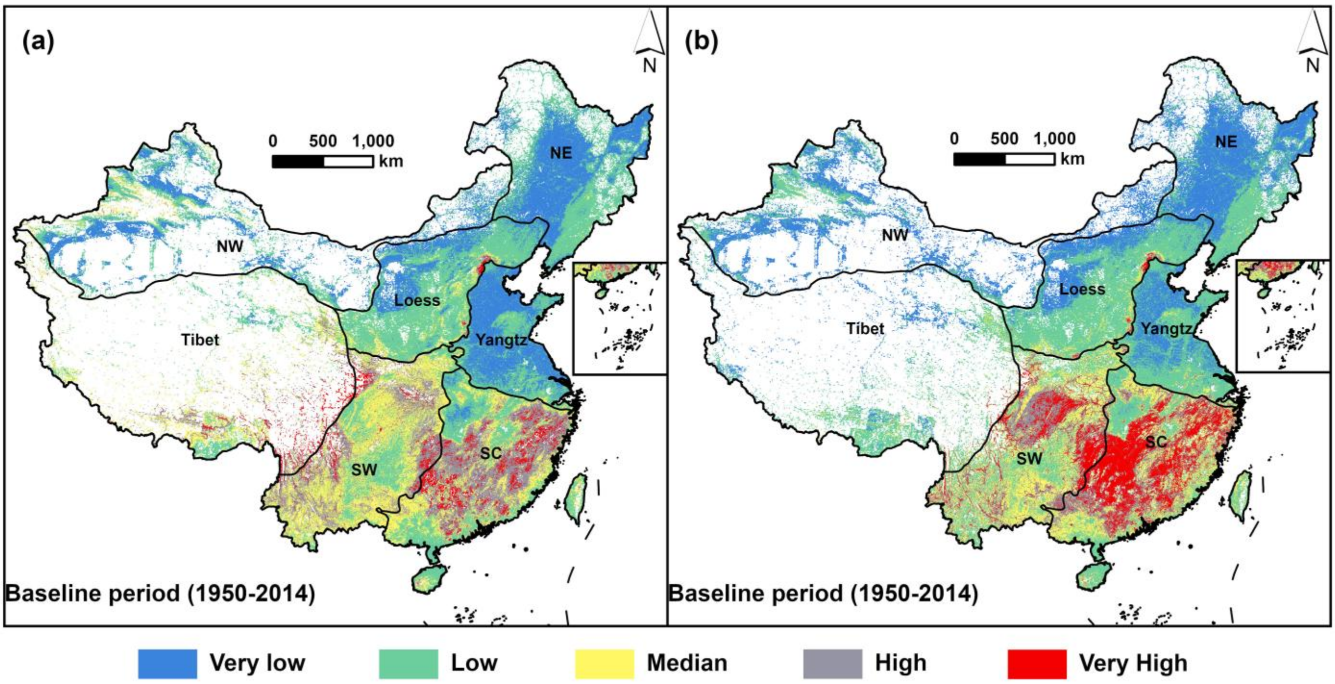

Supplementary Figure. S6: Landslide susceptibility mapping within inhabited areas of China for the baseline period (1950–2014) under different non-landslide sampling strategies. (a) Susceptibility map generated using non-landslide points sampled only from areas with human presence (AUC = 0.96). (b) Susceptibility map generated using non-landslide points sampled across the whole of China (AUC = 0.97).

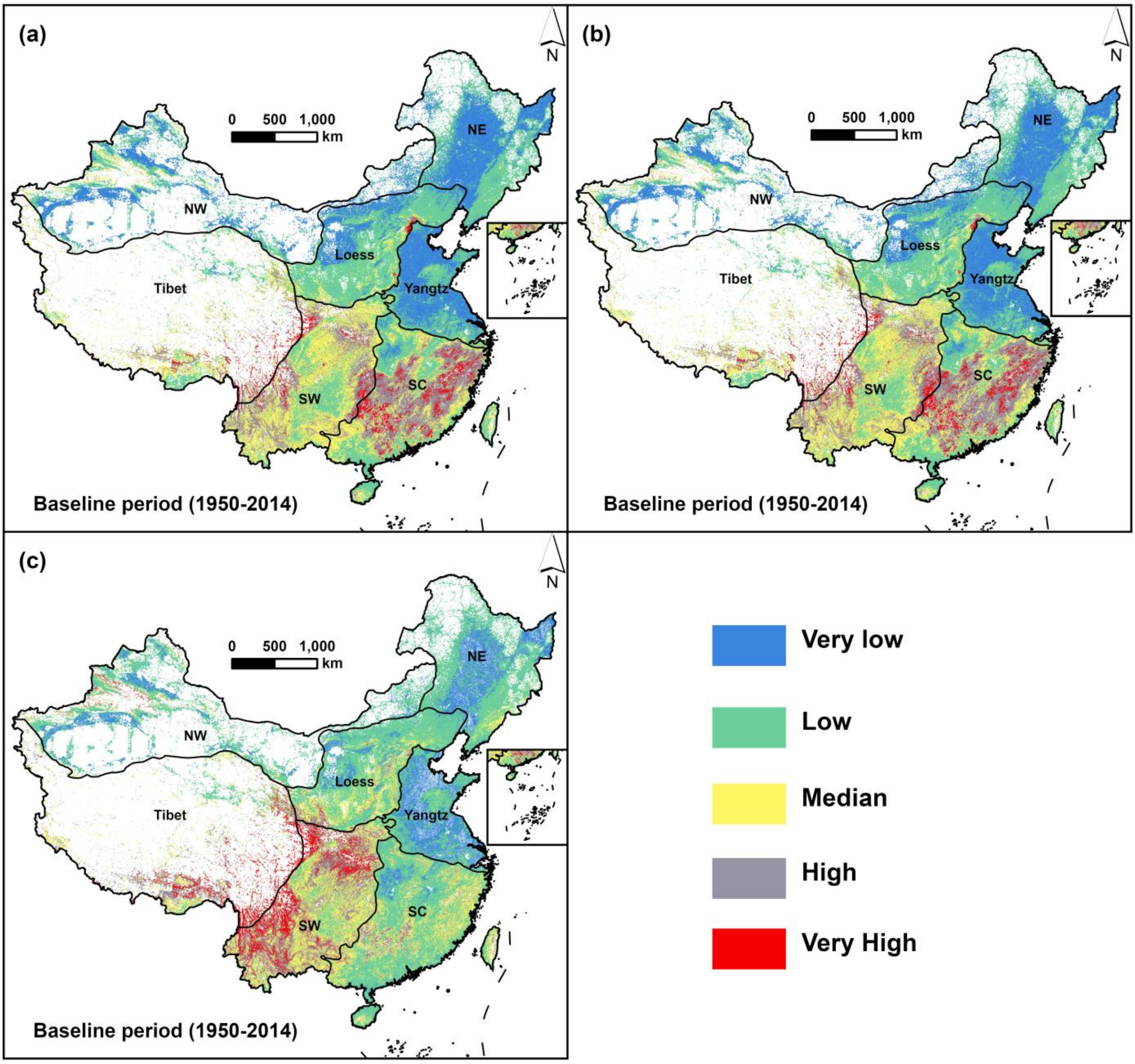

Supplementary Figure. S7: Landslide susceptibility maps illustrating the effect of small-landslide record completeness on model results. (a) Baseline map constructed from the complete inventory (AUC = 0.96); (b) Map after removing 50% of the small landslides from the inventory (AUC = 0.94); (c) Map after completely excluding small landslides from the inventory (AUC = 0.94).

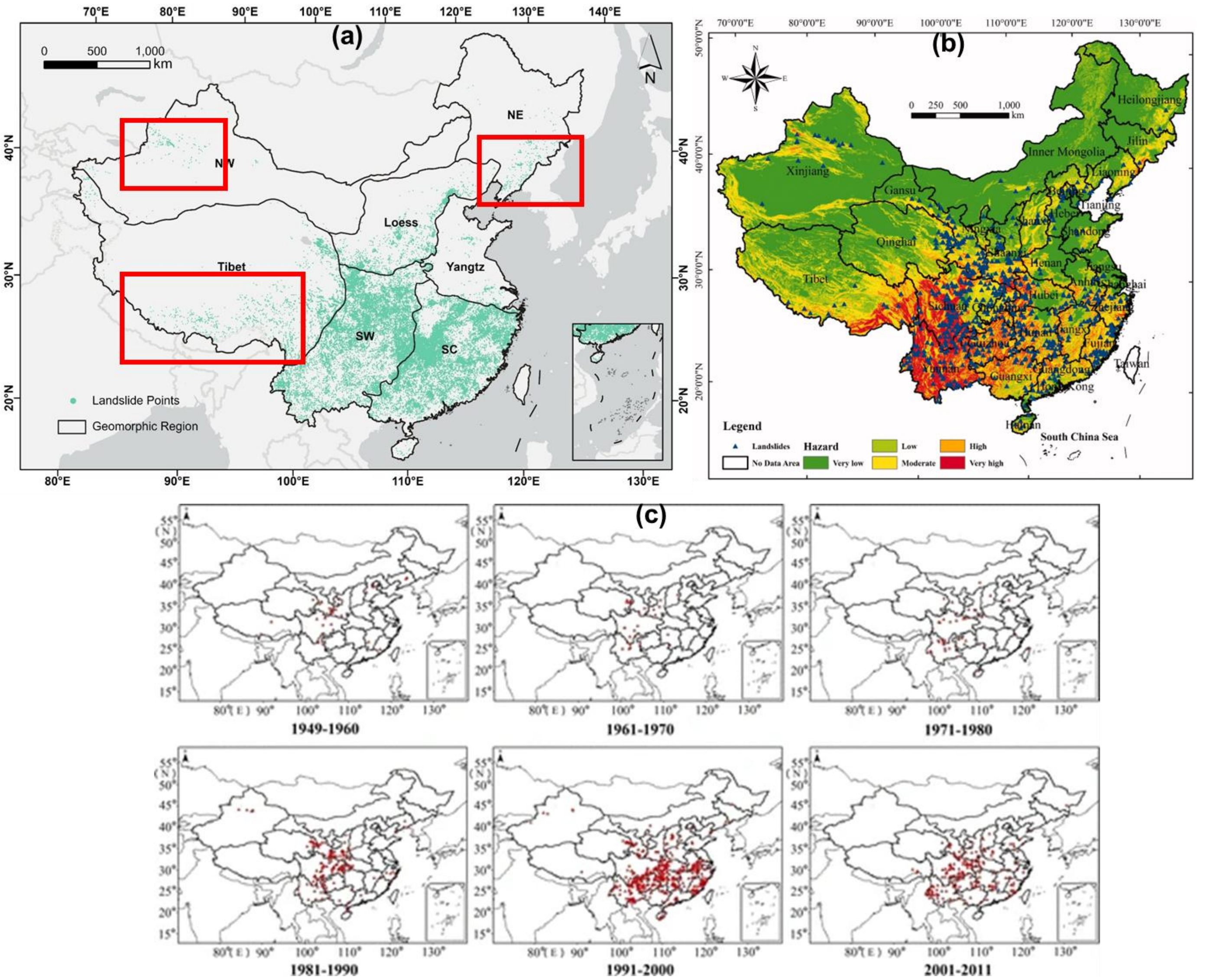

Supplementary Figure. S8: Comparison of landslide inventories. (a) Landslide points used in this study; (b) National-scale landslide inventory from Liu and Miao (2018); (c) National-scale landslide inventory from Liu et al. (2013).

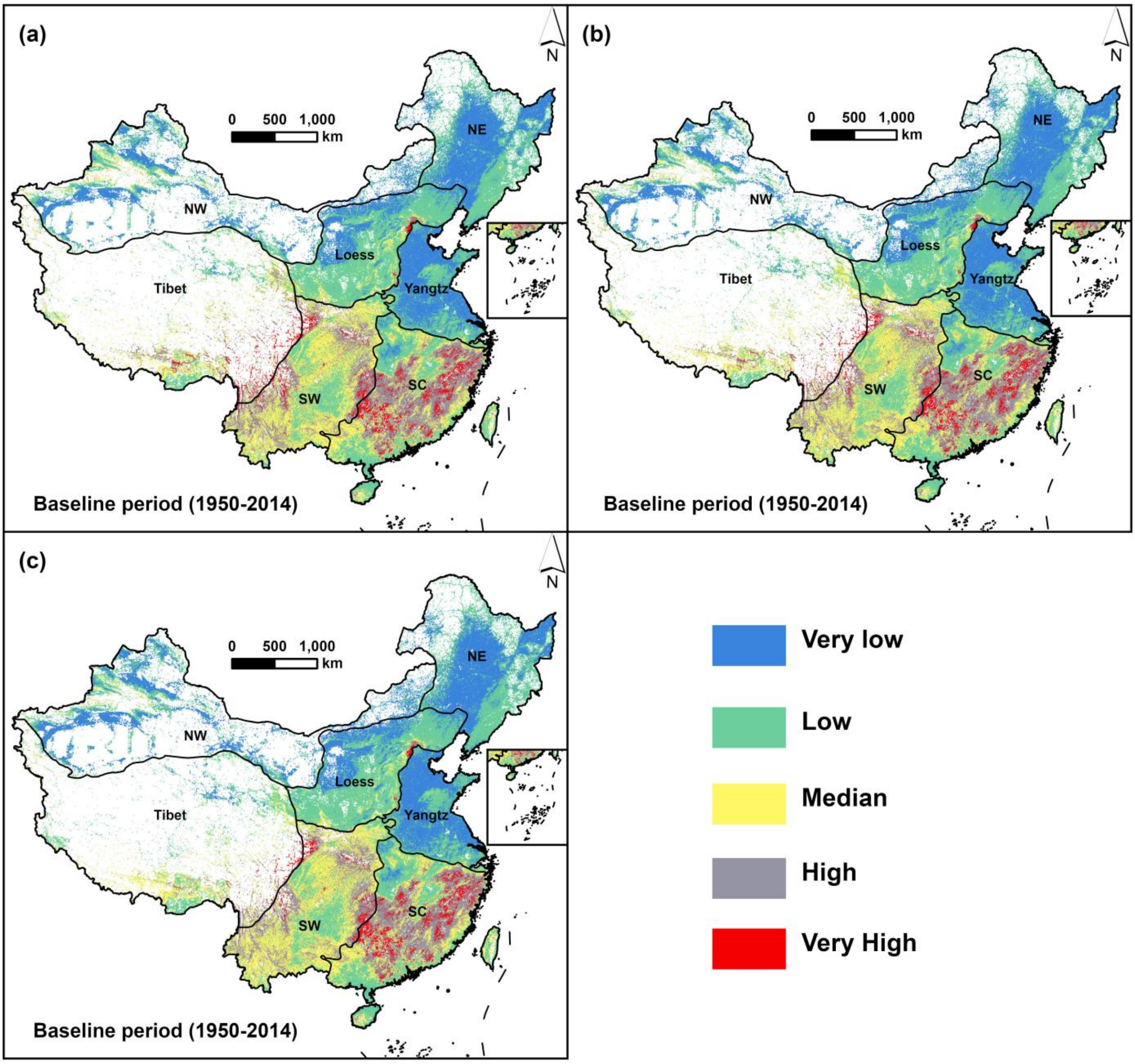

Supplementary Figure. S9: Landslide susceptibility maps generated from inventories with different levels of completeness in Northwest (NW), Northeast (NE), and permafrost region of the Qinghai-Tibet Plateau (Tibet) (AUC = 0.96). (a) Baseline map using the complete inventory; (b) Map after randomly removing 50% of landslide points in the target regions (AUC = 0.96); (c) Map after randomly removing 75% of landslide points in the target regions (AUC = 0.95).

References

Liu, X. and Miao, C.: Large-scale assessment of landslide hazard, vulnerability and risk in China, Geomatics, Natural Hazards and Risk, 9, 1037–1052, https://doi.org/10.1080/19475705.2018.1502690, 2018.

Liu, C., Li, W., Wu, H., Lu, P., Sang, K., Sun, W., Chen, W., Hong, Y., and Li, R.: Susceptibility evaluation and mapping of China's landslides based on multi-source data, Nat Hazards, 69, 1477–1495, https://doi.org/10.1007/s11069-013-0759-y, 2013.